Hybrid Epoxy-Based Thermosets Based on Polyhedral Oligosilsesquioxane: Cure Behavior and Toughening Mechanisms

G.-M. KIM,[1]* H. QIN,[1] X. FANG,[1†] F. C. SUN,[1‡] P. T. MATHER[1,2]

[1]Polymer Graduate Program, University of Connecticut, Storrs, Connecticut 06269

[2]Chemical Engineering Department, University of Connecticut, Storrs, Connecticut 06269

Received 5 April 2003; revised 23 May 2003; accepted 1 June 2003

ABSTRACT: Polyhedral oligosilsesquioxane (POSS)-reinforced thermosets based on octaglycidyl epoxy polyhedral oligosilsesquioxane cured with 4,4′-diaminodiphenyl sulfone (DDS) were prepared and studied for their cure, thermomechanical, and microstructural characteristics. Particular attention was paid to nanometer-scale deformation processes responsible for toughening, as revealed by transmission electron microscopy (TEM) in conjunction with the thermal properties. A cure analysis investigated with calorimetry and rheometry showed a significant dependence of the cure mechanism and kinetics on the DDS content, but all hybrid thermosets reacted completely below 300 °C into rigid solids. A dynamic mechanical analysis of this hybrid resin system showed that increasing the DDS concentration used during cure increased the dynamic storage modulus in the glassy (temperature < glass-transition temperature) and rubbery (temperature > glass-transition temperature) states, simply through an increase in the crosslink density. The phase structures revealed by TEM with selective POSS staining were drastically affected by the DDS concentration and manifested as altered nanomechanical deformation structures. It was qualitatively found that the main toughening mechanism in the studied POSS-reinforced thermosets was void formation at the nanometer scale, possibly templated by limited POSS aggregation. As the crosslinking density increased with the DDS concentration, microshear yielding between voids prevailed, providing a balance of stiffness, strength, and toughness. © 2003 Wiley Periodicals, Inc. J Polym Sci Part B: Polym Phys 41: 3299–3313, 2003
Keywords: hybrid thermosets; POSS; silsesquioxane; toughening mechanism

INTRODUCTION

Epoxy polymers are by far the most commonly used engineering thermosets because of their outstanding mechanical and thermal properties, such as high strength, high modulus, low creep, and reasonable elevated-temperature performance. However, their intrinsic brittleness (i.e., no large-scale plastic deformation before cracking) has imposed severe limitations on their structural applications. As a result, efforts devoted to improving the toughness of thermosets (including epoxies and bismaleimides, among others) have continued to grow for several decades. Most successful strategies concerning the toughening of epoxy resins have involved the incorporation of dispersed elastomeric and thermoplastic

*Present address: Institute for Materials Science, Martin-Luther University Halle-Wittenberg, 06029 Halle/S. Germany

†Present address: Underwriters Laboratories, Incorporated, Northbrook, Illinois 60062

‡Present address: Curriculum in Applied Sciences, University of North Carolina, Chapel Hill, North Carolina 27599

Correspondence to: P. T. Mather (E-mail: patrick.mather@uconn.edu)

Journal of Polymer Science: Part B: Polymer Physics, Vol. 41, 3299–3313 (2003)

phases into the resin matrix, which results in a multiphase polymeric system.[1–3] Numerous investigations have shown that the optimal dispersion of elastic or thermoplastic domains discretely within the matrices of epoxy resins results in a substantial enhancement of the fracture energy or toughness, but with a compromise in both the tensile modulus and glass-transition temperature (T_g). The toughening mechanisms in such composite materials have been reasonably well established in the literature. Specifically, the toughening mechanisms attributed to the presence of such particles includes localized shear deformation in the form of shear bands running between rubber particles[4–7] and internal cavitation,[8,9] or debonding from the matrix, of rubber particles.[4–8] Unfortunately, such methods generally do not provide adequate improvements in toughness for highly crosslinked, high-T_g epoxies and their composites—materials of particular interest for aerospace and automotive applications.

Recently, in response to these challenges, new approaches have been attempted that exploit various organic–inorganic hybrid materials. Because of the broad diversity of molecular structures available in organic–inorganic hybrid materials, these materials frequently exhibit unexpected hybrid properties synergistically derived from both components; that is, a desirable balance of stiffness, strength, and toughness, as well as improved thermal stability, most of which are unique and different from any other traditional composites or blends.[10–13] Examples of such approaches include intercalated and exfoliated montmorillonite clay (aluminosilicate),[10–12,14,15] *in situ* precipitation of an inorganic phase in polar polymeric matrices,[16–18] and single-wall nanotube dispersions.[19] A surprising observation of a simultaneous increase in the flexural modulus and compact tension fracture toughness has been reported for a range of epoxy systems modified with organically modified montmorillonite clay.[20]

A newly developed approach offering a unique level of control involves the use of nanometer-sized hybrid monomers ($R_8Si_8O_{12}$, where R is reactive or not) copolymerized within a polymeric host. Specifically, polyhedral oligosilsesquioxane (POSS) monomers bear a carefully designed cage-like silicate structure with precise polymerization functionality[21,22] that prescribes a homogeneous (nanometer-scale) dispersion of silica-like compositions via polymerization. From a design perspective, POSS monomers and their local aggregates can be considered the small filler particles of conventional polymer composites. However, a difference is that each POSS monomer contains nonreactive organic functionalities for solubility and compatibility with the matrix while precisely maintaining one or more covalently bonded reactive functionalities suitable for polymerization, grafting, and surface bonding. Intensive studies have established that the introduction of such nanostructured POSS monomers within a polymer leads to increases in T_g and the degradation temperature, increased fluid elasticity, improved oxidation resistance, reduced flammability, and modest tensile modulus improvements.[21,23–25] In the area of thermosetting polymers, Choi and coworkers[26,27] showed that octaglycidyl POSS (eight epoxide groups per POSS cage) cured with a common diamine, diaminodiphenylmethane (DDM), resulted in thermomechanical properties and fracture properties quite similar to those of baseline diglycidyl ether of bisphenol A (DGEBA)/DDM epoxies, but with dramatic differences in stiffness above T_g. To our knowledge, these are the only studies of the fracture toughness of POSS-based polymers. Using a distinct POSS–epoxy monomer that had mixed functionality and was cured with an aliphatic diamine, Li et al.[28] observed broadening of the glass transition, modest increases in the glassy modulus, and dramatic increases in the rubber modulus.

Therefore, although considerable effort has been given to the synthesis and processing of these unique polymers, relatively little work has focused on the structure–processing–property relationships in these material systems. To obtain better insight into underlying reinforcement mechanisms, we have tried to discern the exact role of POSS incorporation for a range of polymeric hosts in altering mechanical properties through direct and indirect observation of mechanical deformation. In this work, we have prepared POSS-reinforced epoxy resins based on octaglycidyl epoxy polyhedral oligosilsesquioxane [or octakis(dimethylsiloxypropylglycidyl ether) silsesquioxane (OG–POSS)] cured with various amounts of 4,4′-diaminodiphenyl sulfone (DDS) as a curing agent (a high-performance hardener). We have examined their cure behavior, postcure thermomechanical behavior, and solid-state morphology to identify mechanisms responsible for the improvements of the mechanical properties of these materials and to aid in the interpretation of the thermal and rheological properties.

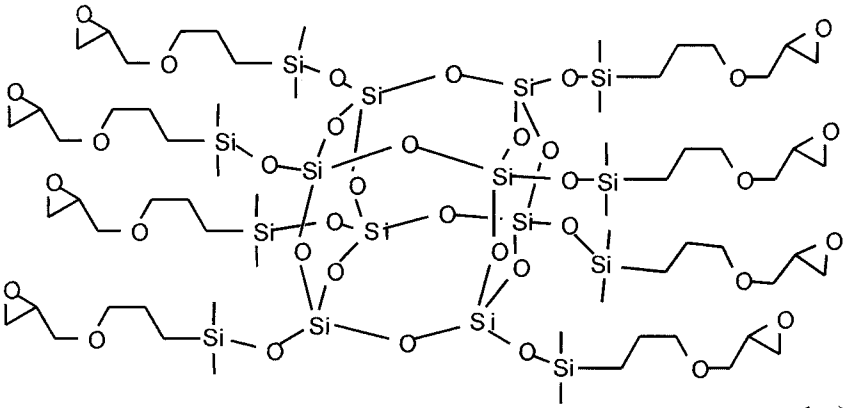

1a)

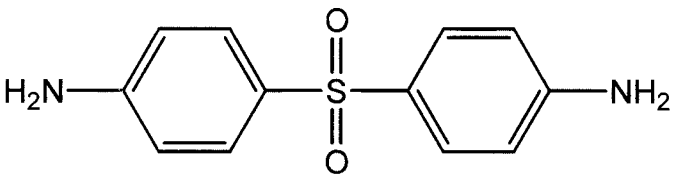

1b)

Scheme 1. Chemical structures of the materials used in this study: (a) OG–POSS and (b) DDS.

EXPERIMENTAL

OG–POSS/DDS Preparation

OG–POSS was purchased from Tal Materials, Inc., and was used after extensive vacuum drying. Its preparation from tetraethoxysilane has been previously described.[26,29] As shown in Scheme 1(a), OG–POSS is octafunctional, possessing eight glycidyl ether groups (epoxides) that are easily reacted with proton-donating groups from primary and secondary amines[26] or from carboxylic acids.

To produce solid epoxy materials, we adopted a procedure detailed here for OG–POSS/DDS with 100% stoichiometry, and, more generally for various mixture ratios. OG–POSS was gradually heated in a glass vial to 180 °C with an oil bath, after which a prescribed amount of DDS (25, 50, 75, and 100% of stoichiometric equivalents), which had reactive hydrogens [Scheme 1(b)], was added; the mixture was mixed manually with a spatula for several minutes under a nitrogen purge. The mixture turned light yellow when DDS melted and partially dissolved within OG–POSS; complete dissolution only occurred later, as the cure ensued. Choi et al.[26] observed a comparatively high solubility of the DDM curing agent in OG–POSS, and we attribute this difference to the higher polarity of DDS afforded by the sulfone linkage. Next, the OG–POSS/DDS mixture was poured into a room-temperature-cured silicone mold (RTV630A/B, GE Silicones) custom-

fabricated for rectangular bar casting and placed in a vacuum oven. A moderate dynamic vacuum was applied while samples were thermally equilibrated at 100 °C. The degassing of the samples was accomplished by repeated oven evacuation and refilling with nitrogen during slow heating to 140 °C. The bubble-free samples were finally heated to 200 °C for 4 h to complete the thermal curing.

A similar procedure was applied to the preparation of DGEBA/OG–POSS/DDS blends; for neat DGEBA/DDS samples, a clear liquid was achieved once the mixture was heated to a temperature higher than 120 °C. DGEBA is a commonly studied diepoxide used for the preparation of epoxy-based thermosets.

Differential Scanning Calorimetry (DSC)

DSC measurements were conducted to measure the curing behavior with a TA DSC2920 under a nitrogen atmosphere. The samples were sealed in aluminum pans and were heated and cooled in the DSC instrument at a rate of 10 °C/min with sample masses of approximately 10 mg. The DSC temperature and heat-flow values were calibrated with an indium standard. The instrument's baseline, measured for empty aluminum pans, was subtracted from the curing runs, and the second run of the cured samples was used as the baseline and subtracted from the first run.

Rheological Measurements

The rheological analysis of the curing reaction of OG–POSS was investigated with a strain-controlled rotational rheometer (ARES, Rheometric Scientific, Inc.) with dynamic oscillations with disposable aluminum fixtures. The thermosetting resins required a particular sample preparation protocol to yield reproducibility via limited precuring. In particular, the OG–POSS resin was heated to 180 °C in a glass vial with an oil bath, after which a prescribed quantity of DDS (25, 50, 75, or 100% of amine hydrogen/epoxide equivalents) was added; the mixture was stirred with a spatula by hand for several minutes. The 10-mm-diameter parallel disks of the rotational rheometer were preheated to 100 °C, and their separation was set to 0.5 mm. Two to three drops of the light yellow mixture (0.05 mL) were added to form a thin layer between the two plates, after which time the temperature was ramped to an isothermal curing temperature (180, 200, or 220 °C) at a rate of 4 °C/min and the linear viscoelastic shear properties were monitored at a single frequency of 10 rad/s. Separate temperature-sweep rheological experiments were conducted on the same materials to quantify the evolution of the viscoelastic properties following a temperature profile similar to that used in the bar manufacturing process. For these experiments, OG–POSS/DDS mixtures were cured in the rheometer while temperature was swept from 100 to 300 °C at a heating rate of 2 °C/min and while linear viscoelastic shear measurements were measured at a frequency of 10 rad/s and with a strain that was adjusted from 10 to 1% to maintain a constant maximum (but small) shear stress in the samples.

Dynamic Mechanical Analysis (DMA)

DMA was used to measure the temperature dependence of the complex tensile modulus with a TA Instruments DMA2980 in a three-point-bending mode. The samples were analyzed over a broad temperature range spanning from −50 to 250 °C with a heating rate of 4 °C/min and with measurements taken every 0.5 °C. A fixed oscillation frequency of 1 Hz was used with a strain of approximately 0.1%. The sample bars were 1 mm thick, 2 mm wide, and 25 mm long.

Morphology and Deformation Processes

Morphological studies were performed with a Philips 300 transmission electron microscope operated at 80 kV. Ultrathin sections about 50 nm thick were prepared by ultramicrotomy with an LKB III microtome equipped with a diamond knife at room temperature. Phase structures were taken from ultrathin sections stained with RuO_4, a staining agent found to be selective for the POSS moiety. For the imaging of deformation structures, the bulk specimens were randomly ultramicrotomed; this process led indirectly to crack creation within the ultrathin sections so that near-crack regions could be directly visualized. In contrast to our study of deformation-free morphology, deformation structures at the crack tip were imaged without any chemical staining treatment.

RESULTS AND DISCUSSION

The curing reactions of OG–POSS with the DDS hardener were studied with DSC, and the results

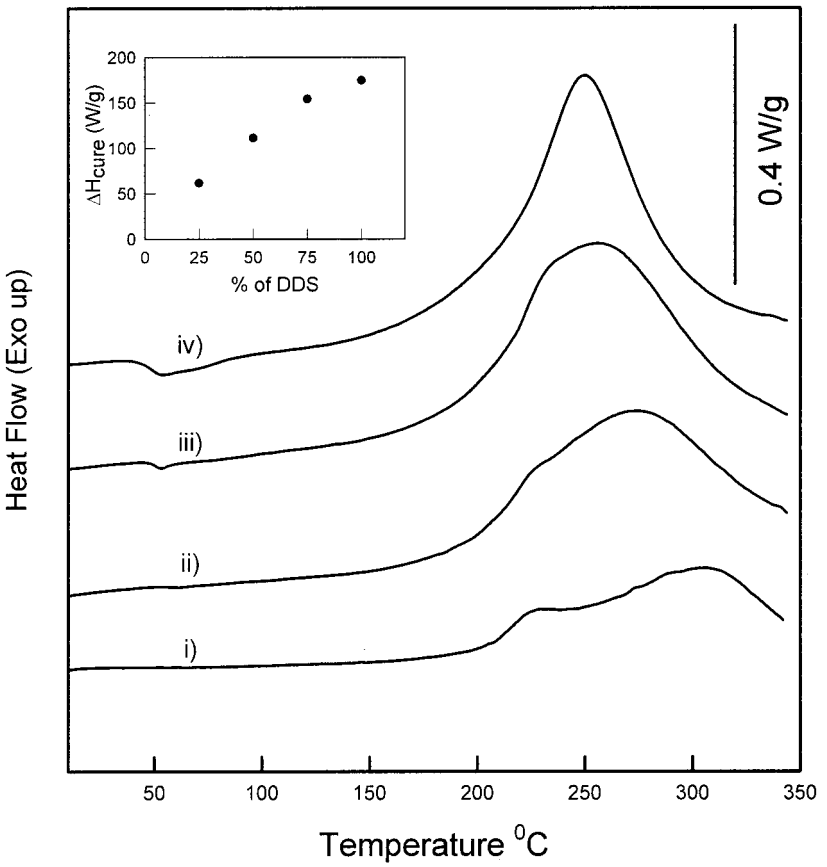

Figure 1. DSC for OG–POSS/DDS epoxies with (i) 25, (ii) 50, (iii) 75, and (iv) 100% of the stoichiometric ratio of DDS. The inset graph shows a plot of ΔH_{cure} versus the stoichiometric ratio of DDS. A heating rate of 10 °C/min was used with a blanket of gaseous nitrogen.

are shown in Figure 1. Because DDS has limited solubility in OG–POSS, especially for temperatures below the melting temperature of 170 °C, the precuring of the materials (before DSC analysis) was needed to produce homogeneous samples. Thus, in the DSC study of the OG–POSS epoxy with different amounts of DDS, all samples were precured at 180 °C under stirring for 15 min, this process yielding clear liquids. Such a process, though necessary, led to uncertainty in the total heat of reaction, as some cure surely transpired under the precure conditions.

We can observe in the heating traces of Figure 1 a significant dependence of the curing behavior on the level of DDS addition, as is commonly observed for a variety of epoxy systems. With 25% of the stoichiometric amount of DDS, our OG–POSS hybrid epoxy shows two exothermic peaks during cure, which suggest that two distinct mechanisms are active. A separate thermal analysis of pure OG–POSS (results not shown) gave no evidence for self-polymerization, so this possibility was ruled out. Instead, we suggest that limited linear chain growth involving two epoxides per POSS and the two primary amines of DDS proceeds with a lower activation energy at low DDS levels, at least in comparison with crosslinking that later proceeds via the two remaining DDS hydrogens (now of secondary amines) and the remaining excess of epoxide groups. As the amount of DDS is increased, the lower temperature exotherm peak shifts to higher temperatures, whereas the higher temperature exotherm peak shifts to lower temperatures. Once the amount of DDS reaches 100% (1 mol of OG–POSS/2 mol of DDS), only one exothermic peak can be observed, revealing an apparently simpler cure mechanism. Importantly, specimens with 75 and 100% of the stoichiometric amount of DDS reveal distinct T_g's near 50 °C, whereas the other

Table 1. Summary of the DSC Data Measured during the Curing of Various Samples: T_g, Temperature of the Maximum Exotherm (T_{EXO}), and ΔH_{cure} of the OG–POSS/DDS Epoxies with Different DDS Stoichiometric Ratios

Sample	Stoichiometry (%)	T_g (°C)	T_{EXO} (°C)	ΔH_{cure} (J/g)
I. OG–DDS-25	25	—	303/229	61.7
II. OG–DDS-50	50	—	275/231	111.4
III. OG–DDS-75	75	50.29	257/240	154.2
IV. OG–DDS-100	100	49.30	248	174.6

samples show no T_g's for temperatures greater than 20 °C. This is a strong indication that significant cure occurs during the precure treatment that leads to a more complete reaction for higher DDS concentrations, as manifested in T_g growth. A summary of the DSC findings gleaned from the traces of Figure 1 for OG–POSS/DDS cure is given in Table 1.

In the case of substoichiometric DDS addition, not all the epoxy groups participate in the cure reaction. On the basis of this argument, we expect a smaller value of the heat of reaction [or curing enthalpy (ΔH_{cure})] for the OG–POSS epoxy with insufficient DDS. The inset in Figure 1 is a plot of ΔH_{cure} resulting from the use of different DDS levels. For the specimens with 25, 50, and 75% DDS, ΔH_{cure} increases linearly. However, the extrapolation of these three data points to 0% DDS does not give an intercept of zero. This may be the result of our precuring of the DSC samples. For the sample with 100% DDS, the curvature is negative. This may also be related to the precuring of the DSC samples. One other possible explanation is that during the late stage of curing, the system gels (particularly so for 100% stoichiometry), so that some of the functional groups cannot diffuse and are trapped in an unreacted form. On the basis of the results from DSC, we can conclude that DDS contributes to the curing process not only as an accelerator but also as a crosslinking site for epoxy groups, as shown in Scheme 2. During the curing reaction, each primary amine of DDS reacts with an epoxy group of OG–POSS, via ring opening, to form a —CH_2—CH(OH)—CH_2— linkage, whose pendant hydroxyl group is known to accelerate subsequent ring-opening reactions. As the curing proceeds, epoxy groups begin reacting with secondary amines and hydroxyl groups in a similar manner, although at a lower rate; the remaining epoxy rings crosslink the polymer chains.

To further understand the curing reaction of OG–POSS with DDS, we conducted a rheological study. Specifically, OG–POSS and different stoichiometric ratios of DDS were preheated to 180 °C and held at that temperature for 6–8 min to achieve optimum miscibility between the two compounds with a minimum curing effect; they were then cooled to 100 °C. Dynamic oscillatory material functions (shear storage modulus, G', shear loss modulus, G'', and complex viscosity $|\eta^*|$) were then collected as functions of the temperature as the temperature was ramped from 100 to 300 °C at 2 °C/min; this thermal history mimicked that of our thermoset bar processing. The results of such temperature sweeps for OG–POSS cured with 25, 50, 75, and 100% DDS (relative to the stoichiometric ratio) are shown in Figure 2.

After a period of low viscosity for all samples (in fact, below the limit of sensitivity for our configuration), the curing reaction accelerates at lower temperatures with an increasing DDS concentration. The curing reaction of OG–POSS with 25% DDS is initiated at 215 °C, with the complex viscosity value beginning a dramatic increase at that point. According to the complex viscosity data, OG–POSS with 50, 75, or 100% DDS begins a rapid cure reaction at 195, 180, or 175 °C, respectively. We note that that the complex viscosity trend for OG–POSS with 100% DDS nearly overlaps the data for 75% DDS at temperatures slightly higher than the starting cure temperature.

The isothermal curing of OG–POSS at various DDS levels was also studied rheologically. Specifically, OG–POSS with 25, 50, 75, or 100% DDS was cured isothermally at 180, 200, or 220 °C. The results of these experiments are shown in Figure 3 (a–d). Importantly, the precure viscosity level is quite low at 10^{-1} Pa s for all samples, in contrast to analogous clay–epoxy systems reported by Brown et al.[30] for which the precure viscosity was observed to increase 1000-fold with the addition of 10 wt % S30A clay (Southern Clay Products, Inc.). As expected from our nonisother-

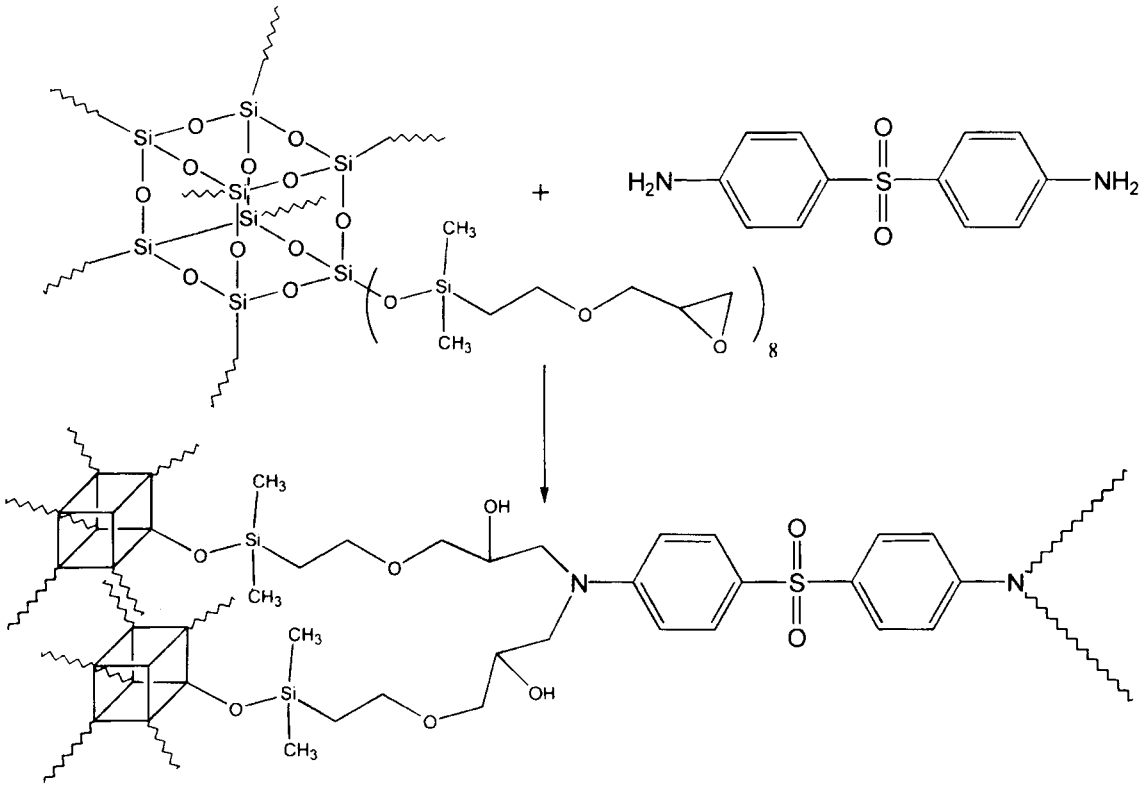

Scheme 2. Postulated reaction of OG–POSS with the four functional groups of DDS (two primary amines and two secondary amines). Such epoxy–amine reactions are commonly autocatalytic in nature because of an accelerating effect of the hydroxyls formed during epoxide ring opening.

mal results, lower cure temperatures lead to longer time requirements that yield the same extent of reaction as observed qualitatively from the asymptotic behavior of the viscosity curve. Moreover, lower DDS percentages in the mixtures also lead to longer cure times, this again being consistent with nonisothermal results. For example, a cure reaction of OG–POSS with 25% DDS at 200 °C requires isothermal heat treatment for 25 min [see Fig. 3(d), trace ii] to nearly complete the cure, whereas OG–POSS cured with 50, 75, or 100% DDS requires isothermal heating periods of 13, 8, or 5 min, respectively [see Fig. 3(a–c)] for the same temperature. For full curing of the materials, at least according to mechanical property development, OG–POSS containing DDS must be treated at 200 °C for at least 4.5 h with 25% DDS, for 2.5 h with 50% DDS, and for less than an hour with 75 or 100% DDS. Therefore, the curing procedure adopted for the characterization of the cured samples by DMA and transmission electron microscopy (TEM) was 4–8 h at 200 °C (see the Experimental section).

To examine the influence of the stoichiometric ratio on the solid-state mechanical properties of cured OG–POSS/DDS epoxies, we used DMA with flexural samples. Figure 4 shows typical DMA data obtained from specimens having various stoichiometric ratios of DDS but fully cured, as discussed previously. Increasing the amount of DDS up to 100% stoichiometry results in a large storage modulus increase for the whole temperature range studied. In particular, the rubbery state modulus (i.e., the storage modulus when the temperature is greater than T_g) strongly increases with the amount of DDS; this finding is related to the crosslinking density.[19] However, we show later that the POSS content is also important in this respect.

We interpret the observed modulus data primarily in terms of the increasing crosslinking density, not in terms of the increasing weight fraction of POSS in the cured materials. Specifically, with an increasing DDS concentration, the crosslinking density increases in the cured network because of the simple addition of crosslink-

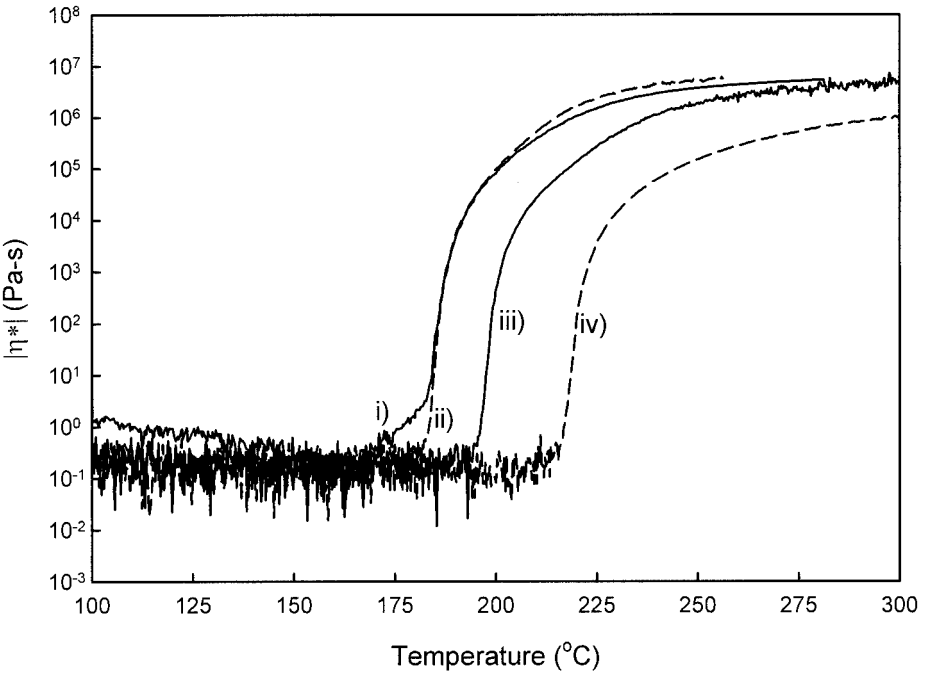

Figure 2. Temperature dependence of the complex viscosity ([η*]) for OG–POSS/DDS epoxies undergoing cure with (i) 100, (ii) 75, (iii) 50,, and (iv) 25% of the stoichiometric ratio of DDS. The heating rate was 2 °C/min, and the oscillation frequency was 10 rad/s.

ing sites due to both primary and secondary amines. During the cure of epoxies, crosslinking reactions continue until vitrification for relatively low-temperature cures or until reactant diffusion is sufficiently retarded in the rubbery network to quench the reaction rate to zero.[31] Figure 4 indicates that, with an increasing amount of DDS, T_g shifts to higher temperatures. Moreover, this shift in T_g occurs with a concomitant rise in the rubber modulus so that the net result of these two effects is a modulus curve with a comparatively small modulus drop at the transition. This result may be partially attributed to the incorporation of POSS within the thermoset, especially the increase in the rubber modulus. The most distinctive feature of each DMA trace in Figure 4 is the α transition, or glass transition, for each epoxy, and this transition loses strength, as indicated by the loss tangent peak magnitude decreasing, with increasing DDS content. Aside from the α transition, cured materials with DDS in the 75–100% range reveal weak secondary relaxation (β relaxation) peaks from 0 to 50 °C. We attribute their presence to crankshaft rotations of glycerol units [—CH_2—CH(OH)—CH_2—O—] that appear in greater concentrations with epoxide ring-opening reactions via DDS amines (Scheme 2) and thus with the DDS concentration. We note that such a β relaxation has frequently been shown to depend on such factors as the formulation stoichiometry and degree of cure.

The DMA characterizations of the flexural specimens was also carried out for OG–POSS, DGEBA epoxy resins, and their blends, all cured with stoichiometric quantities of DDS, for comparison with a standard epoxy formulation. Specifically, each epoxide ring was balanced with one amine hydrogen in all the formulations. In Figure 5, traces i and iii belong to the DGEBA/DDS and OG–POSS/DDS epoxy resins. Trace ii belongs to a blend containing a 50:50 (w/w) ratio of DGEBA to OG–POSS, still preserving the epoxide/hydrogen stoichiometry. Figure 5 shows that the DGEBA/DDS epoxy resin has the highest T_g, approximately 250 °C. The OG–POSS/DDS epoxy, however, has the lowest T_g at 150 °C, and the 50:50 blend shows a T_g of 200 °C, precisely between that of the two extremes. We attribute the relatively low T_g value of the OG–POSS samples to the large concentration of dimethylsiloxane groups in the materials; this is an aspect that can be easily remedied by the use of POSS materials featuring more rigid linkages between the epoxide functionality and the silsesquioxane core.

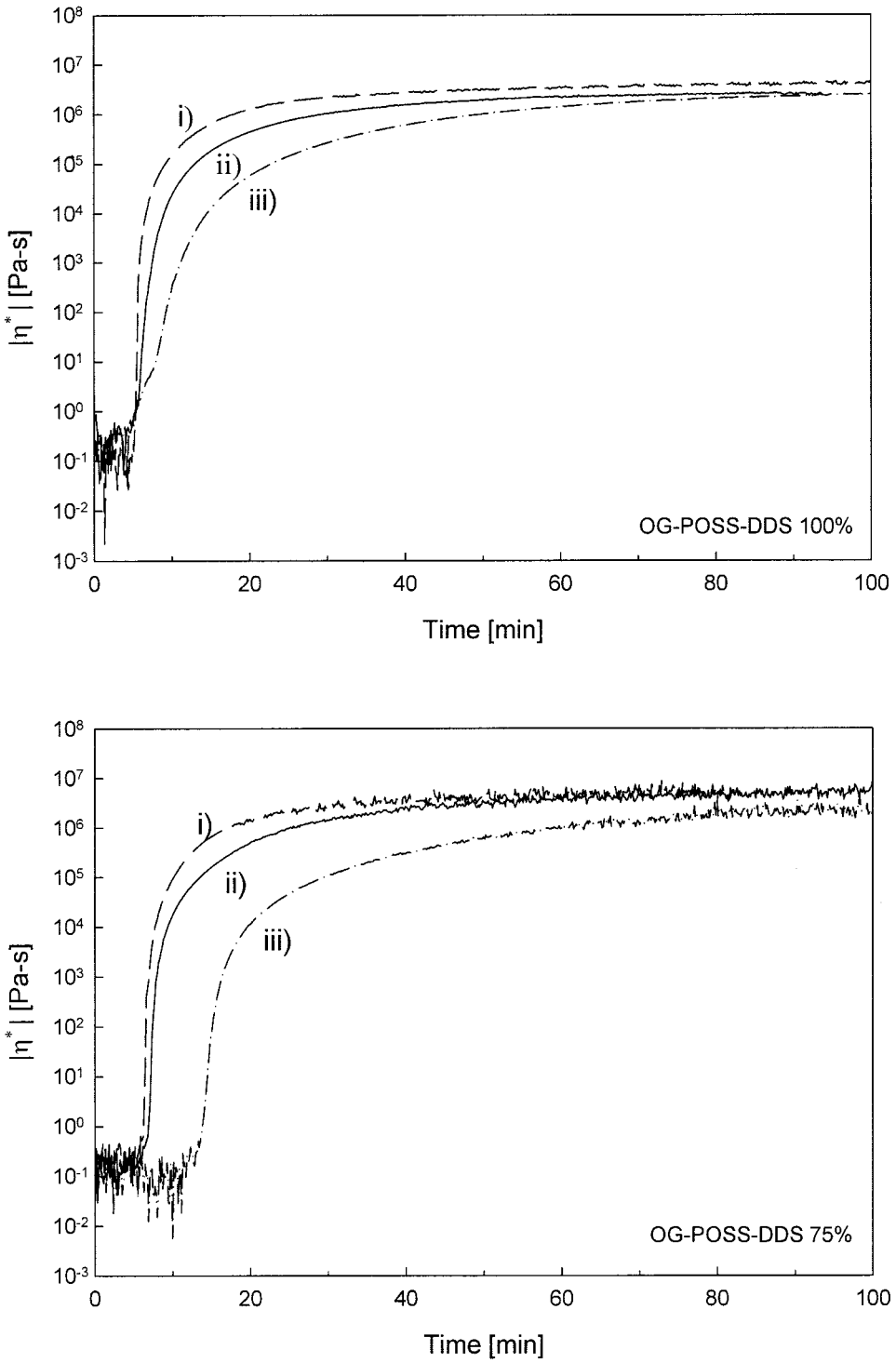

Figure 3. Evolution of the complex viscosity ([η^*]) measured at a frequency of 10 rad/s during the isothermal curing of OG–POSS/DDS epoxies with different amounts of DDS at (i) 220, (ii) 200, and (iii) 180 °C. The stoichiometric percentage of DDS used is indicated in each plot.

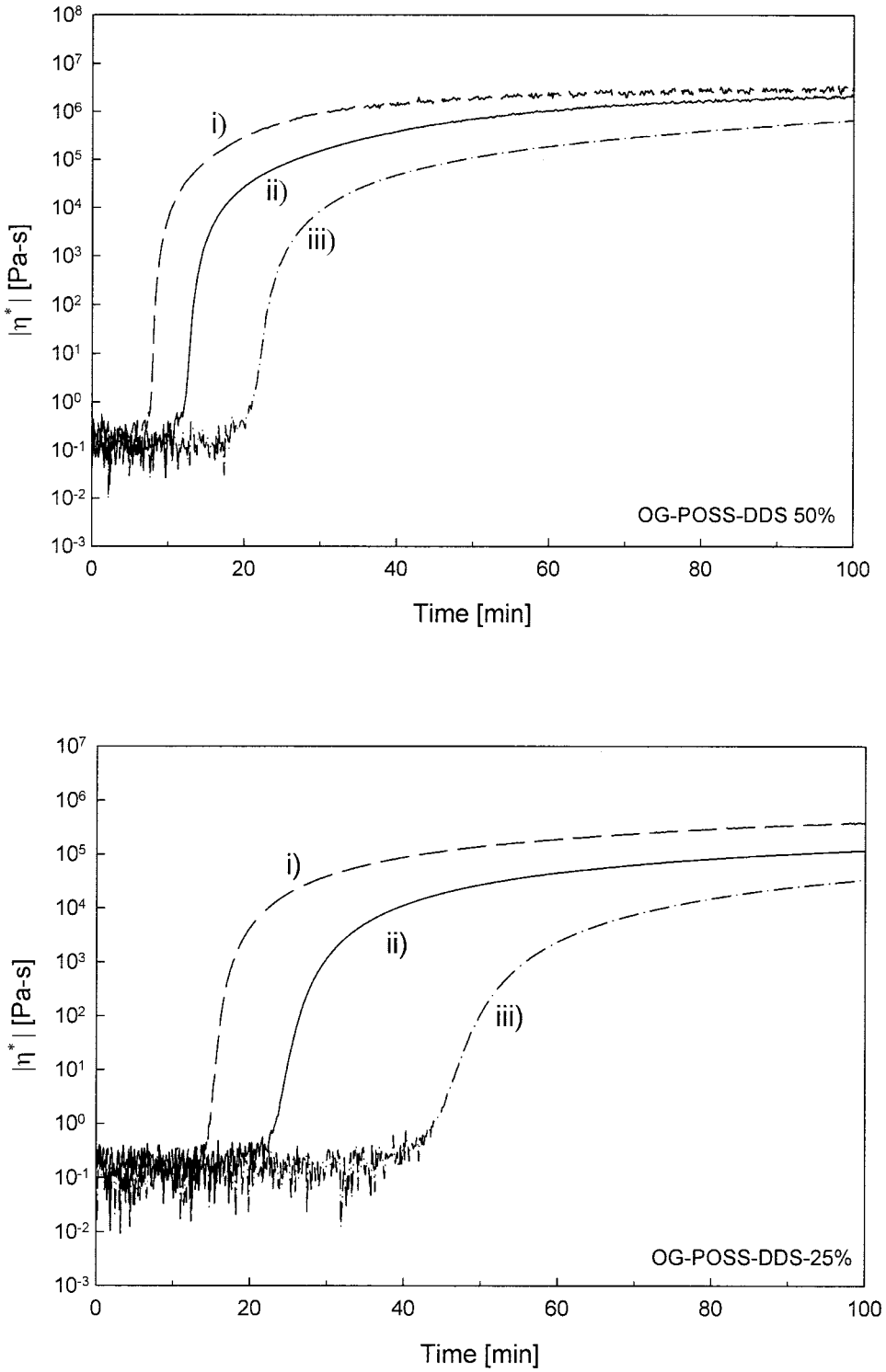

Figure 3. (*Continued from the previous page*)

A comparison of the rubbery moduli above T_g is equally revealing. From the storage modulus traces in Figure 5, we can observe that the OG–POSS/DDS epoxy has a high rubbery modulus around 500 MPa, whereas the DGEBA/DDS epoxy, despite stoichiometric and complete cure, has

a much lower rubbery plateau of 30 MPa. The 50:50 blend features a rubbery modulus of 50 MPa, which indicates that the blending of OG–POSS into the DGEBA epoxy can raise the rubbery modulus only modestly. The results further suggest that, through the modification of the OG–POSS structure for an intrinsically higher T_g in the cured form, epoxies with nearly flat modulus–temperature traces should be possible.

In light of the thermomechanical properties that we observed for the OG–POSS/DDS epoxies, we sought to understand the underlying microstructure in the materials. Although the samples were optically quite clear, it was not apparent whether the OG–POSS molecules were so homogeneously mixed and dissolved as to be molecularly dispersed. With this in mind, we examined ultramicrotomed and stained samples of the materials (for the preparation details, see the Experimental section) with TEM. Figure 6 shows the phase structures of OG–POSS cured with different stoichiometric ratios of DDS. It should be emphasized that without any staining treatment, no structural distinction or contrast can be recognized with TEM imaging, even as the DDS amount is varied. However, after staining treatment with RuO_4, which is selective for POSS, the phase structures are clearly revealed in TEM micrographs.

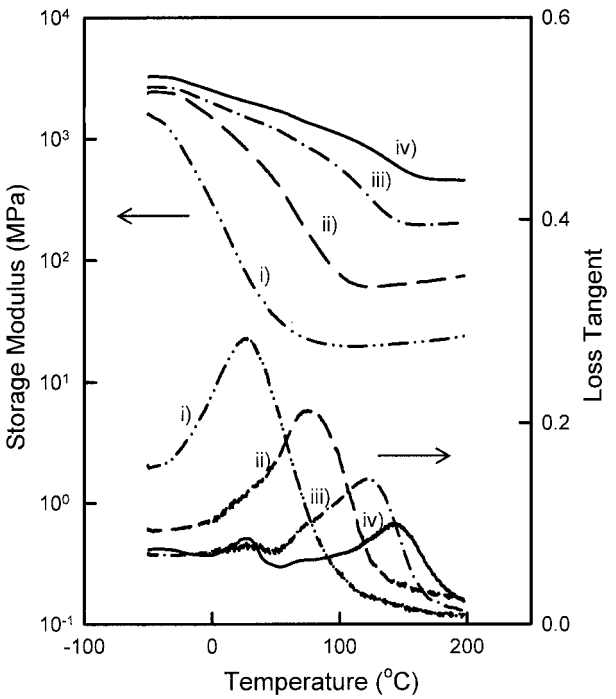

Figure 4. Tensile storage modulus and loss tangent of OG–POSS/DDS epoxies with (i) 25, (ii) 50, (iii) 75, and (iv) 100% of the stoichiometric ratio of DDS. A three-point-bending geometry was used with an oscillation frequency of 1 Hz and a heating rate of 4 °C/min.

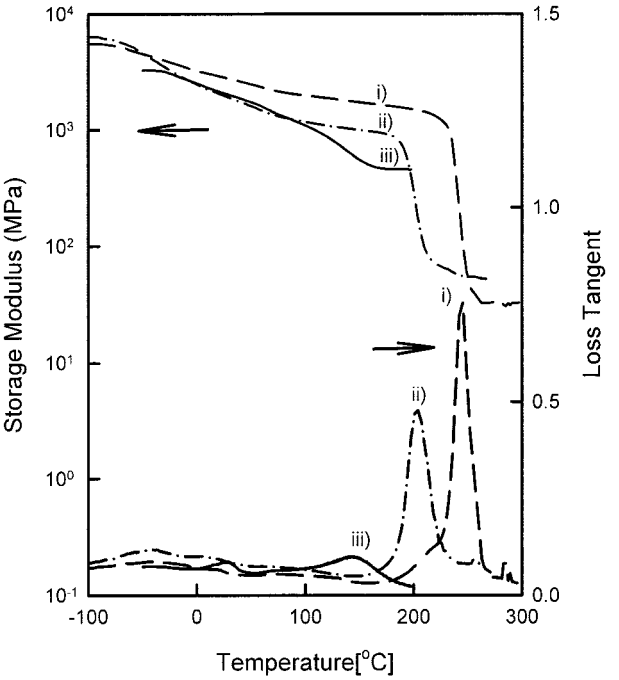

Figure 5. Tensile storage modulus and loss tangent for (i) DGEBA/DDS, (ii) OG–DGEBA (50:50 w/w)/DDS, and (iii) OG–POSS/DDS. A stoichiometric ratio of epoxide to amine was used. The conditions are described in Figure 4.

As expected from the high optical clarity of our samples and from DMA analysis, OG–POSS molecules are well dispersed in the matrix, but a number of dark spots appear at 15 nm and smaller. On the basis of their size, such dark spots should consist of aggregated POSS moieties. With increasing amounts of DDS in the OG–POSS system, the phase structure becomes slightly more homogeneous and continuous, with a well-defined and highly crosslinked network structure resulting. We attribute this trend toward homogeneity to an associated increase in the fraction of epoxides per OG–POSS that react and perhaps, therefore, disrupt POSS–POSS associations. We cannot test this hypothesis, however, with the limited observations made so far. Nevertheless, the POSS aggregates that we have observed are well dispersed at a nanometer scale in the thermoset network. We note that the POSS aggregate size does not change with the concentration of DDS; rather, the aggregate concentration increases

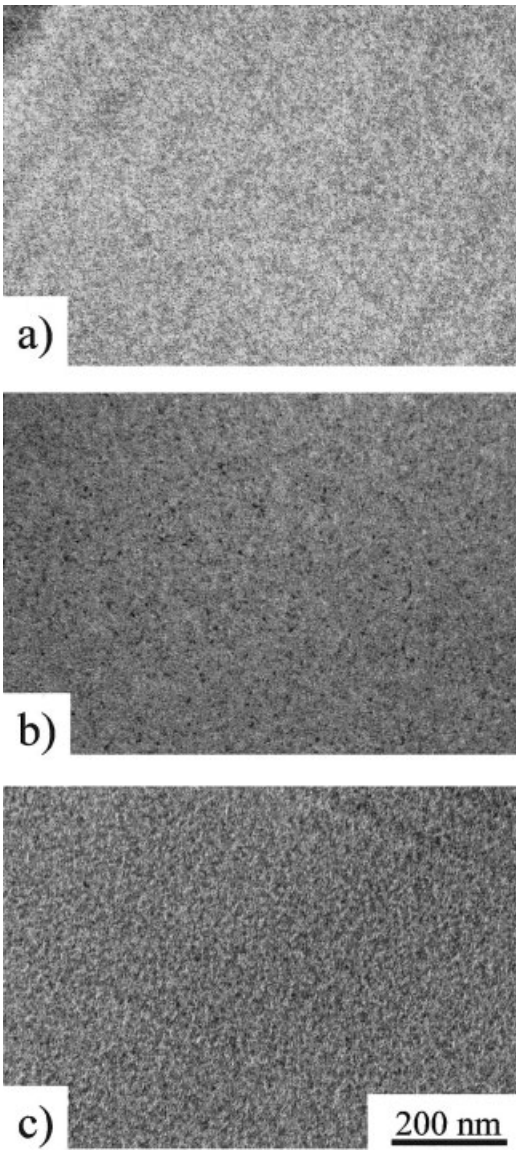

Figure 6. TEM micrographs revealing the phase structures of OG–POSS/DDS epoxies with (a) 50, (b) 75, and (c) 100% of the stoichiometric ratio of DDS. The samples were stained with RuO_4 and microtomed to a thickness of approximately 50 nm.

with the amount of DDS. Surely, this particular morphology, neither molecular-dispersion-like nor fillerlike, is relevant in determining the ultimate mechanical properties. Additionally, the results from our TEM study on phase structures give us direct observations of POSS aggregates with chemical staining with RuO_4; to our knowledge, this is the first successful staining of POSS for imaging purposes.

As mentioned previously, the phase structures of OG–POSS/DDS epoxies are altered by the concentration of DDS and are expected to influence the mechanical deformation processes. To test this idea, we examined thin-film deformation zones near cracks existing in microtomed sections. Figure 7 shows our findings for deformation structures selected from many observations as typical and indirectly generated by the random microtoming of bulk samples.

The near-crack TEM images show well-developed plastic deformation zones at the crack tips. With increasing DDS, the plastic deformation zone becomes more diffuse and broadened. In par-

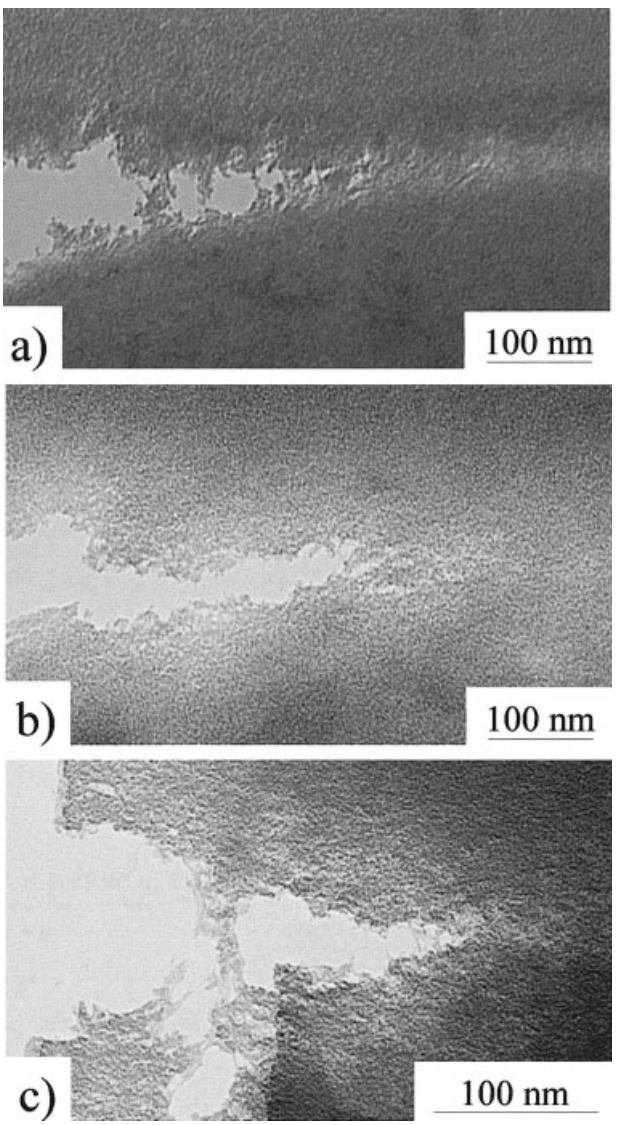

Figure 7. TEM micrographs revealing deformation structures of OG–POSS/DDS epoxies with (a) 50, (b) 75, and (c) 100% of the stoichiometric DDS ratio. The samples were stained with RuO_4 and randomly microtomed; this caused damage that could be visualized.

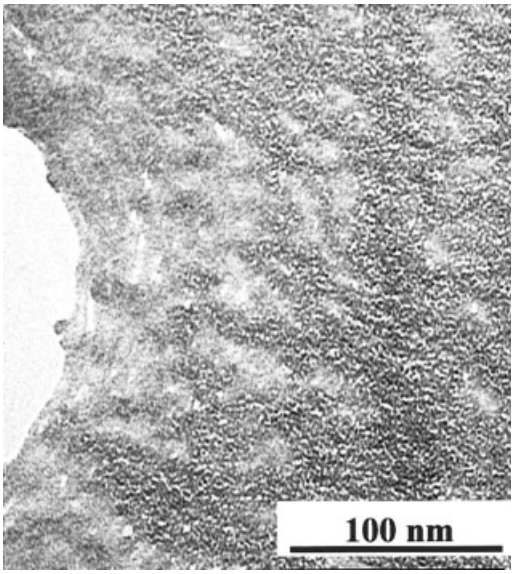

Figure 8. Representative deformation structure taken from an OG–POSS epoxy with 100% of the stoichiometric ratio of DDS. The image contrast was enhanced with Adobe Photoshop to highlight the apparent aggregation structures.

ticular, in the more completely crosslinked case (100% DDS), some fibrils bridge both sides of an opened crack. Shown in Figure 8 is another representative deformation structure for OG–POSS with 100% DDS; the contrast has been enhanced to more clearly show the nanometer-scale heterogeneity as it interacts with near-crack deformation.

This figure reveals a well-developed void formation with an 8–12-nm dimension in the matrix surrounding the POSS moieties within the plastic zone ahead of the crack tip. The presence of such voids reduces the local buildup of hydrostatic stress at the crack tip and allows some shear yielding to occur around their vicinity in the matrix. Furthermore, nanovoids at the crack tip strongly interact with the yielding of the material in the front of the crack tip, blunting the cracks in the plastic deformation zone. The initiation of nanovoids and their subsequent growth should enhance matrix shear yielding, which is directly associated with energy dissipation during deformation; that is, it is reflected in the enhancement of the toughness of the materials. In comparison with the deformation of thermoplastics, the molecular mobility in highly crosslinked epoxies is restricted so that plastic deformation (e.g., crazing) is not possible. Furthermore, in OG–POSS epoxies, the POSS moieties exist at least partially as nanoscale aggregates strongly bonded to the matrix, obviating traditional cavitation from hard inclusions.[32–35] Thus, as a result of the initiation of voids in the matrix caused by the presence of POSS aggregates (clearly shown in Fig. 8), plastic shear bands are increasingly initiated with increased DDS content. Consequently, considerably more plastic energy may be dissipated during fracture with increasing DDS content. In other words, as the crosslinking density increases with the DDS concentration, microshear yielding between the voids predominates.

Figure 9 schematically represents the deformation process of the POSS-reinforced thermosets studied in this work and perhaps other POSS-based thermosets. This process can be described as a three-stage mechanism, which was proposed by Kim and Michler[36] for a different system: semicrystalline polypropylene filled with rubber particles. Despite the significant differences between that system and POSS-based epoxies, we believe that they share some common features in terms of the deformation sequence that we are now describing. In the first step, the presence of POSS aggregates causes the generation of stress concentrations around them in the matrix. Second, because of the high crosslinking density and strong anchoring of POSS aggregates to the cured system, the network structure cannot maintain continuity under an external load. The highly concentrated stress can only be released by the formation of voids surrounding the POSS aggregates in the matrix. In the third stage, with the growth of voids orthogonal to the principal tensile stress direction, the shear yielding of the matrix is induced in the form of shear bands. Although the growth of the voids themselves may dissipate only a small portion of the energy, a far more important aspect of this process is that it enables shear yielding of the matrix to be activated. The main contribution to the fracture energy increase in the POSS-reinforced thermosets studied is thus argued to be the shear yielding mechanism in the matrix triggered by void formation templated by POSS nanoaggregates.

CONCLUSIONS

In this work, we prepared POSS-reinforced thermosets based on OG–POSS with DDS to study the relationship between the thermal and rheological properties and the nanoscopic deformation pro-

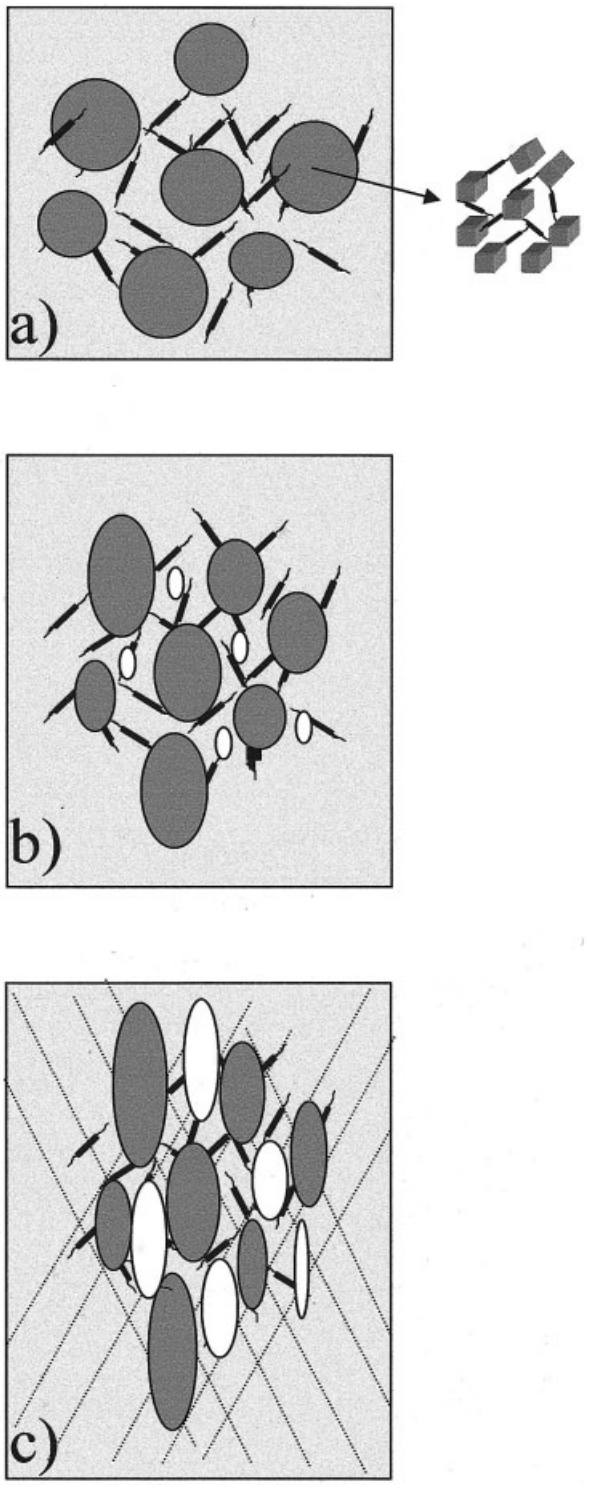

Figure 9. Schematic deformation process: (a) undeformed stage, (b) earlier stage of plastic deformation under a tensile load, and (c) advanced stage of plastic deformation. In parts b and c, the light regions represent nucleated voids.

cesses, particularly those responsible for toughening mechanisms.

A thermal analysis has shown that with an increasing amount of DDS as a curing agent, T_g of the cured OG–POSS system shifts to higher temperatures, and the storage modulus increases below and above T_g. TEM studies of the phase structure have shown that as the amount of DDS in the OG–POSS system increases, the resulting phase structure becomes more homogeneous and continuous, but it has persistent 8–12-nm POSS-rich aggregates. It can be concluded from the TEM imaging of near-crack regions that deformation is initiated by the presence of POSS aggregates and results in localized shear deformation in the form of shear bands spanning POSS aggregates, with subsequent plastic growth of voids in the epoxy matrix. This diffuse shear yielding near a growing crack, combined with a large concentration of small local plastic deformation events, may provide an effective means of absorbing a large amount of strain energy, which can, in turn, be used to effectively toughen a brittle or notch-sensitive polymer. Further examination of such toughening on macroscopic samples is needed to rigorously test this idea.

REFERENCES AND NOTES

1. Bucknall, C. B. Toughened Plastics; Applied Science: London, 1977.
2. Kinloch, A. J.; Young, R. J. Fracture Behavior of Polymers; Applied Science: London, 1983.
3. Rothon, R. Particulate-Filled Polymer Composites; Longman: Essex, 1995.
4. Kinloch, A. J.; Shaw, S. J.; Tod, D. A.; Hunston, D. L. Polymer 1983, 24, 1341–1354.
5. Yee, A. F.; Pearson, R. A. J Mater Sci 1986, 21, 2462–2474.
6. Huang, Y.; Kinloch, A. J.; Bertsch, R. J.; Siebert, A. R. Toughened Plastics I; Advances in Chemistry Series 233; American Chemical Society: Washington, DC, 1993.
7. Huang, Y.; Kinloch, A. J. J Mater Sci Lett 1992, 11, 484–487.
8. Parker, D. S.; Sue, H. J.; Huang, J.; Yee, A. F. Polymer 1990, 32, 2267–2277.
9. Okamoto, Y.; Miyagi, H.; Mitsui, S. Macromolecules 1993, 26, 6547–6551.
10. Usuki, A.; Kawasumi, M.; Kojima, Y.; Kurauchi, T.; Kamigaito, O. J Mater Res 1993, 8, 1174–1178.
11. Giannelis, E. P. Adv Mater 1996, 8, 29–35.

12. Kim, G.-M.; Lee, D.-H.; Hoffmann, B.; Kressler, J.; Stöppelmann, G. Polymer 2001, 42, 1095–1100.
13. Mather, P. T.; Jeon, H. G.; Romo-Uribe, A.; Haddad, T. S.; Lichtenhan, J. D. Macromolecules 1999, 32, 1194–1203.
14. Vaia, R. A.; Giannelis, E. P. Macromolecules 1997, 30, 8000–8009.
15. Wang, Z.; Pinnavaia, T. J. Chem Mater 1998, 10, 3769–3771.
16. Ahmad, Z.; Mark, J. E. Chem Mater 2001, 13, 3320–3330.
17. Deng, Q.; Moore, R. B.; Mauritz, K. A. Chem Mater 1995, 7, 2259–2268.
18. Young, S. K.; Jarrett, W. L.; Mauritz, K. A. Polymer 2002, 43, 2311–2320.
19. Haggenmueller, R.; Gommans, H. H.; Rinzler, A. G.; Fischer, J. E.; Winey, K. I. Chem Phys Lett 2000, 330, 219–225.
20. Becker, O.; Varley, R.; Simon, G. Polymer 2002, 43, 4365–4373.
21. Haddad, T. S.; Lichtenhan, J. D. Inorg J Organomet Polym 1995, 5, 237–246.
22. Lichtenhan, J. D. Commun Inorg Chem 1995, 17, 115–130.
23. Lichtenhan, J. D.; Noel, C. J.; Bolf, A. G.; Ruth, P. N. Mater Res Soc Symp Proc 1996, 435, 3–11.
24. Haddad, T. S.; Lichtenhan, J. D. Macromolecules 1996, 29, 7302–7304.
25. Romo-Uribe, A.; Mather, P. T.; Haddad, T. S.; Lichtenhan, J. D. J Polym Sci Part B: Polym Phys 1998, 36, 1857–1872.
26. Choi, J.; Harcup, J.; Yee, A. F.; Zhu, Q.; Laine, R. M. J Am Chem Soc 2001, 123, 11420–11430.
27. Laine, R. M.; Choi, J.; Lee, I. Adv Mater 2001, 13, 800–803.
28. Li, G. Z.; Wang, L.; Toghiani, H.; Daulton, T. L.; Koyama, K.; Pittman, C. U., Jr. Macromolecules 2001, 34, 8686–8693.
29. Sellinger, A.; Laine, R. M. Chem Mater 1996, 8, 1592–1593.
30. Brown, J. M.; Curliss, D.; Vaia, R. A. Chem Mater 2000, 12, 3376–3384.
31. Saunders, K. J. Organic Polymer Chemistry; Chapman & Hall: New York, 1988.
32. Yorkgitis, F. M.; Eiss, N. S., Jr.; Willkes, G. L.; McGrath, J. F. Adv Polym Sci 1985, 72, 79–109.
33. Kambour, R. P. Polymer 1964, 5, 143–155.
34. Bucknall, C. B.; Smith, R. R. Polymer 1965, 6, 437–446.
35. Donald, A. M.; Kramer, E. J. J Mater Sci 1982, 17, 1871–1879.
36. Kim, G.-M.; Michler, G. H. Polymer 1998, 39, 5689–5697.